N93-29641

RADIATION MODEL PREDICTIONS AND VALIDATION USING LDEF SATELLITE DATA*

T. W. Armstrong and B. L. Colborn
Science Applications International Corporation
Route 2, Prospect, TN 38477
Phone: 615/468-2603, Fax: 615/468-2676

SUMMARY

Predictions and comparisons with the radiation dose measurements on LDEF by thermoluminescent dosimeters have been made to evaluate the accuracy of models currently used in defining the ionizing radiation environment for low Earth orbit missions. The calculations include a detailed simulation of the radiation exposure (altitude and solar cycle variations, directional dependence) and shielding effects (three-dimensional LDEF geometry model) so that differences in the predicted and observed doses can be attributed to environment model uncertainties. The LDEF dose data are utilized to assess the accuracy of models describing the trapped proton flux, the trapped proton directionality, and the trapped electron flux.

INTRODUCTION

Radiation dosimetry data from the Long Duration Exposure Facility (LDEF) mission are being utilized to evaluate the accuracy of current ionizing radiation environment models and to identify model improvements needed for future mission applications in low Earth orbit. A calculational program is in progress to compare model predictions with the different types of LDEF ionizing radiation measurements (dose, activation, LET spectra, secondary particles, etc.), and the status of this work is summarized in a companion paper (ref. 1).

The scope of the present paper is restricted to model predictions and comparisons with LDEF thermoluminescent dosimetry (TLD) measurements of the radiation dose. These TLD measurements provide one set of data for evaluating the accuracy of environment models describing the trapped proton flux, the trapped proton directionality, and the trapped electron flux. Assessments of trapped radiation models utilizing other LDEF data sets from plastic nuclear track detectors and activation sample measurements of induced radioactivity are in progress.

*Work supported by NASA Marshall Space Flight Center, Huntsville, AL, Contracts NAS8-38770 and NAS8-39386.

CALCULATIONAL METHOD

Environment Model -- Results from the calculations of Watts, et al. (ref. 2) are used to model the LDEF exposure to trapped protons. These calculations are based on the standard AP8 omnidirectional proton flux model (ref. 3), with altitude and solar cycle variations during the LDEF mission included, and with the MSFC anisotropy model (ref. 4) applied to determine the trapped proton directionality. In the calculations here, the directionality was taken into account by using different incident energy spectra along directions defined by a 3-D angular grid of 720 equal solid angle intervals about the dose point. Example spectra are shown in Fig. 1.

Spacecraft Model -- The LDEF radiation dosimetry data is influenced by material shielding effects due to the dosimeter itself, nearby components and experiments, and the spacecraft structure. It is necessary to isolate shielding effects particular to the LDEF spacecraft so that the evaluated model uncertainties can be attributed to the ambient radiation environment and so that the results have applicability to other missions with different spacecraft configurations. To help ensure that differences between predictions and measurements are due to the external radiation environment and not shielding effects, a detailed three-dimensional geometry/mass model of the LDEF spacecraft and selected experiment trays has been developed (ref. 5), and this 3-D model has been used to take into account shielding effects for the dose predictions here.

Radiation Transport -- Three-dimensional radiation transport calculations were performed using the 3-D LDEF geometry/mass model and the solid angle sectoring approximation, in which the solid angle around each dose point is divided into small sectors and the shielding attenuation along "ray" directions through each sector is computed. Transport calculations using different trapped proton energy spectra for each direction were carried out using the MSFC code written by Burrell (ref. 6), which employs the straightahead approximation together with fits to stopping power and range relations to obtain an analytical solution of the transport equation. The attenuation is computed for material along each ray direction representing a solid angle sector, the attenuated fluence spectrum is folded with the stopping power for tissue, and the results summed for all rays to obtain the tissue dose.

An example TLD shielding distribution used in computing the radiation attenuation is shown in Fig. 2. Shown are areal densities (aluminum equivalent) along rays emanating at the midpoints of 720 equal solid angle bins surrounding the TLD. The TLD in this case is located in one of the canisters containing tomato seeds in tray F2 (SEEDS experiment, Exp. No. P0004). The outward directed TLD normal is at $\varphi = 240°$ and $\theta = 90°$, where $+\varphi$ is measured from south (row 6) and $+\theta$ from the zenith direction. Also indicated in Fig. 2 is the constant shielding corresponding to a spherical geometry model having a radius equal to the vertical (minimum) TLD shielding, which is the simple geometry model assumed for some of the scoping

estimates in the LDEF pre-recovery dose predictions (ref. 7). As evident, the spherical geometry model substantially underestimates the dosimetry shielding.

RESULTS

TLD measurements were made at various locations on the LDEF spacecraft and at various shielding depths in the experiment trays. Fig. 3 summarizes the TLD data presently available at the larger shielding depths ($\geq$ 0.5 g/cm^2) where trapped protons dominate the dose contribution. The data shown are from dosimeters located: (a) on the trailing (west) side of the spacecraft, consisting of the measurements by Frank, et al. (ref. 8) for TLDs located in experiment tray F2 (Exps. P0004 and P0006), measurements by Frank, et al. (ref. 8) and Reitz (ref. 9) in tray C2 (Exp. A0015), and measurements by Bourrieau (ref. 10) in tray B3 (Exp. A0138-7); (b) on the earth-end of the spacecraft, consisting of measurements by Frank, et al. (ref. 8) and Reitz (ref. 9) in tray G2 (Exp. A0015); and (c) on the leading (east) side, consisting of measurements by Frank, et al. (ref. 8) in tray F8 (Exp. M0004) and by Blake and Imamoto (ref. 11) in tray D9 (Exp. M0003). In two cases, the Exp. M0006 measurements of Chang, et al. (ref. 12) and some of the Exp. M0003 measurements of Blake and Imamoto (ref. 11), TLD assemblies were located in drawers of the experiment trays which were closed 40 weeks into the mission. Thus, the shielding changed during flight in these cases, and results from these measurements are not included in Fig. 3.

The doses in Fig. 3, and in subsequent graphs of this type, are plotted as a function of the "vertical" shielding thickness in g/cm^2 of aluminum equivalent material (based on equivalent ranges for 100-MeV protons), where the vertical direction is along the normal from the TLD face outward from the LDEF interior. This vertical direction generally corresponds to the direction of minimum shielding, although there are exceptions, such as for the TLDs located near the edge of the thick detector stack in Exp. P0006.

Predicted doses and comparisons with the data of Fig. 3 are given below with the objective being to evaluate the accuracy of models describing the magnitude of the trapped proton flux and its angular dependence. Subsequent comparisons using previous predictions (ref. 7) are then made with the TLD data at thin shielding depths where the dose contribution is dominated by incident electrons to assess the accuracy of trapped electron flux models.

Trapped Proton Dose

Figs. 4-6 compare predicted and measured doses for TLDs in LDEF experiment trays located on the trailing edge, earth end, and leading edge of the spacecraft, respectively. Predictions for Exps. P0004 and P0006 located in tray F2 and Exp. M0004 in tray F8 are based on a detailed geometry modeling of the tray

contents (ref. 4); for other cases (trays B3, C2, and G2) the tray contents were modeled as a single homogenized material (aluminum) with reduced density, so the dosimetry shielding is approximate for these cases. For the TLDs located in the Exp. P0006 detector stack, both measurements and calculations show appreciable variation of the dose for different locations within the TLD array for the same vertical shielding depth; the computed doses shown for P0006 are for a point in the middle of the array, and the measured values are the minimum values observed (ref. 9) across the array. The values shown for the Reitz measurements in Exp. A0015 are averages of the reported data (ref. 8) for TLD types 100 and 700.

A summary of the predicted and measured doses is given in Fig. 7. These results show that the AP8 trapped proton flux model gives a lower dose than observed from TLD measurements aboard LDEF for all spacecraft locations and shielding depths, with the predictions usually about a factor of two lower than measured. The predicted-to-measured dose ratios are practically constant with shielding depth, indicating that the trapped proton model environment is too low by about the same factor over a wide range of proton energies. Since the total mission dose is accumulated during the early high-altitude portion of the flight, which occurred predominately during the solar minimum phase of the solar cycle (ref. 2), these conclusions refer to the solar minimum version (AP8MIN) of the AP8 trapped proton model. (Model comparisons with available LDEF induced radioactivity measurements, ref. 13, for relatively short half-life radioisotopes should enable a check of the AP8MAX model since the latter part of the flight took place during solar maximum.)

The present dose predictions based on a detailed LDEF geometry model and an anisotropic trapped proton environment differ from early scoping estimates (ref. 7) made as part of the LDEF pre-recovery predictions in which simple geometry models (sphere and planar) and an omnidirectional trapped proton environment model were used. The difference is illustrated in Fig. 8 for comparisons with the TLD data of Exps. P0004 and P0006. While the omnidirectional, spherical geometry calculations (fortuitously) agree with the data, the more accurate models give doses about a factor two lower than the measurements. This illustrates that directional effects and a reasonably detailed spacecraft geometry model are needed in utilizing LDEF data for definitive assessments of uncertainties in the radiation environment.

Trapped Proton Anisotropy

For the low inclination (28.5°) of LDEF orbits, the dose from galactic cosmic rays is very small due to geomagnetic shielding, and, except for near-surface shielding depths where the trapped electron environment is important, the absorbed dose measurements on LDEF are due almost entirely to the trapped proton exposure during passes through the South Atlantic Anomaly (SAA). In the SAA region at LDEF altitudes, protons are "mirroring" in the geomagnetic field, with trajectories confined mainly in planes perpendicular to the local magnetic field direction and with in-plane asymmetry due to the east-west effect.

Since LDEF had a very stable orientation during the entire mission, measurements at various positions around the spacecraft provide data for evaluating the proton anisotropy model used.

In several cases TLD dosimeters at similar shielding depths were located near the trailing (row 3) and leading (row 9) edges of the spacecraft. These data and predictions in terms of the ratio of trailing-to-leading edge doses are shown in Fig. 9. The measured anisotropy is generally higher than predicted by the MSFC anisotropy model; e.g., the measured anisotropy for Exps. P0004/M0004 and Exps. P0006/M0004 is a factor of ≈ 2.4, whereas the calculated anisotropy factor for these cases is ≈ 1.4.

To further investigate the difference found between measured and predicted trapped proton directionality, several calculations were performed to determine the influence of spacecraft geometry on the predicted anisotropy. Fig. 10 shows the angular variation of dose at a particular depth (4 g/cm^2) for three assumed geometries: (a) the curve labeled "LDEF" was computed using the three-dimensional LDEF spacecraft model, (b) the curve labeled "Cylinder" was computed for a cylindrical spacecraft geometry having the same diameter, length, and total mass as LDEF but with the mass uniformly distributed within the cylinder, and (c) the "Plane" curve is for a planar shielding geometry with infinite backing and lateral dimensions and with the plane normal vector pointed in the plotted direction. These results for different model geometries show significantly different characteristic shapes for the angular variation of the dose. The detailed 3-D spacecraft model exhibits a local enhancement of the dose on the east side of the spacecraft, which is not present for the homogeneous cylinder or planar models. This dose "bump" on the east side is due to the fact that the interior of LDEF underneath the experiment trays contains relatively little mass, so the high flux incident on the west side "streams" through the hollow interior and contributes to the dose on the east side. This radiation streaming through the interior of LDEF can also influence the anisotropy observed at different shielding depths because at deeper depths on the east side the west-side flux contribution becomes larger. This is illustrated in Fig. 11 where the dose at various depths is calculated around the center ring of the spacecraft structure using the 3-D LDEF model. At small depths (e.g., 0.5 g/cm^2) the west side dose is higher, at about 10 g/cm^2 depth the west and east side doses are about the same, and at larger depths (e.g., 14 g/cm^2), corresponding roughly to the bottom of most of the experiment trays, the east side dose is higher.

While these calculations on geometry effects do not fully explain the difference found between the measured and predicted dose anisotropy, they do indicate that the observed anisotropy can be substantially influenced by the spacecraft configuration and that a realistic spacecraft geometry model is necessary in interpreting the measurements and in applying the data to other spacecraft configurations for future missions.

Trapped Electron Dose

Two experiments on LDEF contained TLDs with sufficiently thin shielding that the response is dominated by incident electrons. Measured TLD doses for these cases have been reported by Blake and Imamoto (ref. 11) for Exp. M0003 and by Bourrieau (ref. 10) for Exp. A0138-7. Results from these measurements are plotted in Fig. 12 together with the pre-recovery predictions made by Watts (ref. 7) using the AE8MIN and AE8MAX trapped electron environment models (ref. 14). The predictions are for a planar shield with infinite backing, which is expected to be an adequate geometry approximation in this case because of the shallow shielding penetration of the electrons and secondary bremsstrahlung. The M0003 results reported by Blake and Imamoto for dose in the TLD lithium fluoride have been multiplied by 1.25, the stopping power ratio of water to lithium fluoride for electrons in the applicable energy range, to compare with the calculated results in terms of tissue dose. M0003 measurements were also made for thinner shielding than shown in Fig. 12, but these data points are not included here because, as discussed by Blake and Imamoto, the results are suspect at present due to possible TLD saturation effects.

Fig. 12 shows that for small shielding depths where the incident electron flux is predicted to clearly dominate the dose ($\lesssim 0.1$ g/cm^2, corresponding to $\lesssim 15$ mils of aluminum shielding), there is general agreement between the predictions and measurements. The largest difference is at a shielding depth of about 0.04 g/cm^2, where the predicted dose is lower than measured by a factor of two; near 0.01 g/cm^2, the predicted dose is higher by a factor of 1.5. Blake and Imamoto (ref. 11) point out that the flattening of the measured dose profile near 2×10^4 rads for very thin shielding may be due to TLD saturation effects caused by very high doses in a thin layer of the TLD near the outboard surface and by the steep dose gradient within the TLD thickness. Thus, this may account for at least part of the difference between measurements and predictions in the thin shielding region $\lesssim 3 \times 10^{-2}$ g/cm^2 of Fig. 12 rather than environment modeling uncertainties.

CONCLUSIONS

Based on the radiation dose measurements by thermoluminescent dosimeters on LDEF, the AP8 proton model at solar minimum (AP8MIN) underpredicts the trapped proton flux in low Earth orbit by about a factor of two. This difference between measurement and prediction is not totally unexpected since a factor of two uncertainty is often associated with the AP8 model, but the difference here is larger than indicated by some Shuttle measurements (e.g., ref. 15). The higher radiation dose observed for TLDs on the trailing edge of the spacecraft is in agreement with calculations using the MSFC model for describing the angular dependence of the trapped proton environment, although the measured dose anisotropy, based on the relatively few trailing-to-leading edge TLD positions onboard at common shielding depths, is somewhat

higher than predicted. For thin shielding where incident electrons dominate the dose, predictions based on the AE8MIN trapped electron flux model are in general agreement with the TLD measurements (within a factor of two). Some of this difference may be due to saturation effects in the TLDs, which is still under investigation (ref. 11).

These conclusions should be regarded as tentative since additional calculations and comparisons with other LDEF radiation data are still in progress. For example, measurements of the induced radioactivity in various metal samples, some located in close proximity to the TLDs, provide additional data for evaluating the trapped proton flux model and will allow a cross-check of the conclusions here based on model comparisons with TLD data. Also, a more detailed mapping of the proton anisotropy is available from activation measurements, and these data are expected to provide a more definitive test of the trapped proton anisotropy model. These and other model comparisons with the LDEF ionizing radiation data are underway.

REFERENCES

1. Armstrong, T. W. and Colborn, B. L.: Future Directions for LDEF Ionizing Radiation Modeling and Assessments. Second LDEF Post-Retrieval Symposium, NASA CP-3194, 1993.

2. Watts, J. W.; Armstrong, T. W. and Colborn, B. L.: Revised Predictions of LDEF Exposure to Trapped Protons. Second LDEF Post-Retrieval Symposium, NASA CP-3194, 1993.

3. Sawyer, Donald W. and Vette, James I.: AP-8 Trapped Proton Environment for Solar Maximum and Solar Minimum. National Science Data Center, Goddard Space Flight Center, NSSDC/WDC-A-R&S 76-06, Dec. 1976.

4. Watts, J. W., Jr.; Parnell, T. A. and Heckman, H. H.: Approximate Angular Distribution and Spectra for Geomagnetically Trapped Protons in Low-Earth Orbit, in: *High Energy Radiation Background in Space,* Proc. AIP Conf., Vol. 186, pp. 75-85, American Institute of Physics, New York, 1989.

5. Colborn, B. L. and Armstrong, T. W.: Development and Application of a 3-D Geometry /Mass Model for LDEF Satellite Ionizing Radiation Assessments. Second LDEF Post-Retrieval Symposium, NASA CP-3194, 1993.

6. Burrell, M. O.: The Calculation of Proton Penetration and Dose Rates, George C. Marshall Space Flight Center, Huntsville, AL., NASA TM X-53063, August 1964.

7. Watts, J. W., Jr.: Predictions of LDEF Fluxes and Dose Due to Geomagnetically Trapped Protons and Electrons, in: Ionizing Radiation Exposure of LDEF (Pre-Recovery Estimates), E. V. Benton, et al., *Nucl. Tracks Radiat. Meas.* 20, 75 (1992).

8. Frank, A. L.; Benton, E. V.; Armstrong, T. W. and Colborn, B. L.: Absorbed Dose Measurements and Predictions on LDEF. Second LDEF Post-Retrieval Symposium, NASA CP-3194, 1993.

9. Reitz, G.: Preliminary Total Dose Measurements on LDEF. *Adv. Space Res.*, 12, No. 2, 369 (1992).

10. Bourrieau, J.: LDEF Dosimetric Measurement Results (AO 138-7 Experiment). Second LDEF Post-Retrieval Symposium, NASA CP-3194, 1993.

11. Blake, J. B. and Imamoto, S. S.: A Measurement of the Radiation Dose to LDEF by Passive Dosimetry. Second LDEF Post-Retrieval Symposium, NASA CP-3194, 1993.

12. Chang, J. Y.; Giangano, D.; Kantorcik, T.; Stauber, M. and Snead, M.: Thermoluminescent Dosimetry for LDEF Experiment M0006. First LDEF Post Retrieval Symposium, NASA CP-3134, 1992.

13. Harmon, B. A.; Fishman, G. J.; Parnell, T. A. and Laird, C. E.: Induced Activation Study of LDEF. Second LDEF Post-Retrieval Symposium, NASA CP-3194, 1993.

14. Vette, James I.: The AE-8 Trapped Electron Model Environment. National Space Science Data Center, Goddard Space Flight Center, NSSDC/WDC-A-R&S 91-24, Nov. 1991.

15. Richmond, R. G.; Badhwar, G. D.; Cash, B. and Atwell, W.: Measurement of Differential Proton Spectra Onboard the Space Shuttle Using a Thermoluminescent Dosimetry System, *Nucl. Instr. Meth.* A256, 393 (1987).

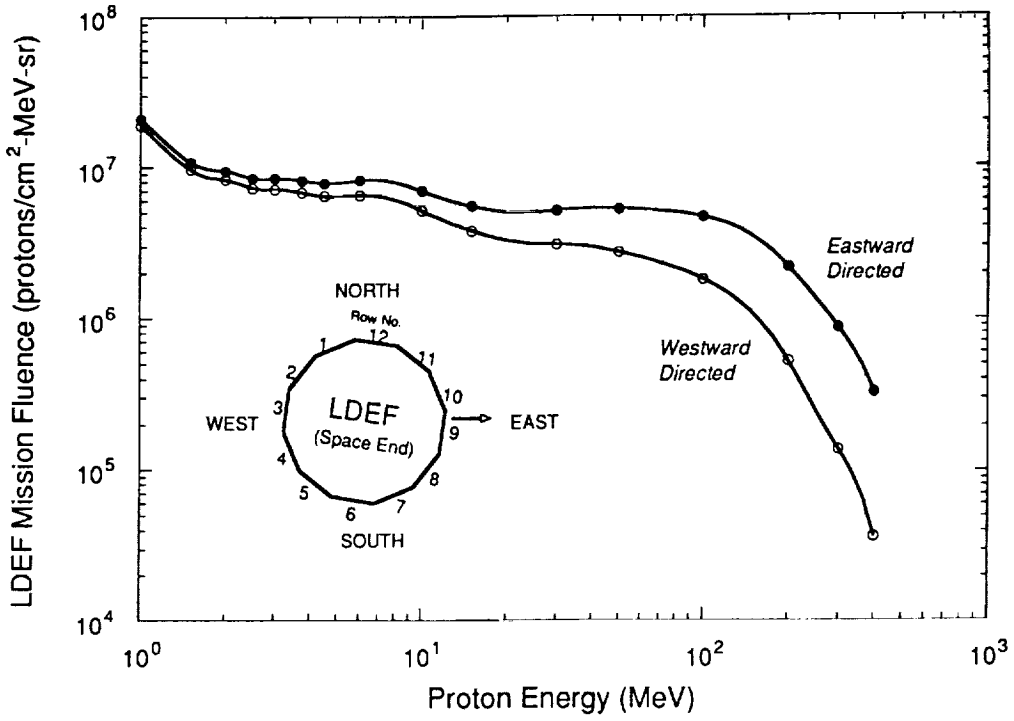

Figure 1. Directionality of LDEF radiation exposure to trapped proton environment. Example fluence spectra are shown for only two directions, the eastward-directed fluence (incident on west side of LDEF) and the westward-directed fluence.

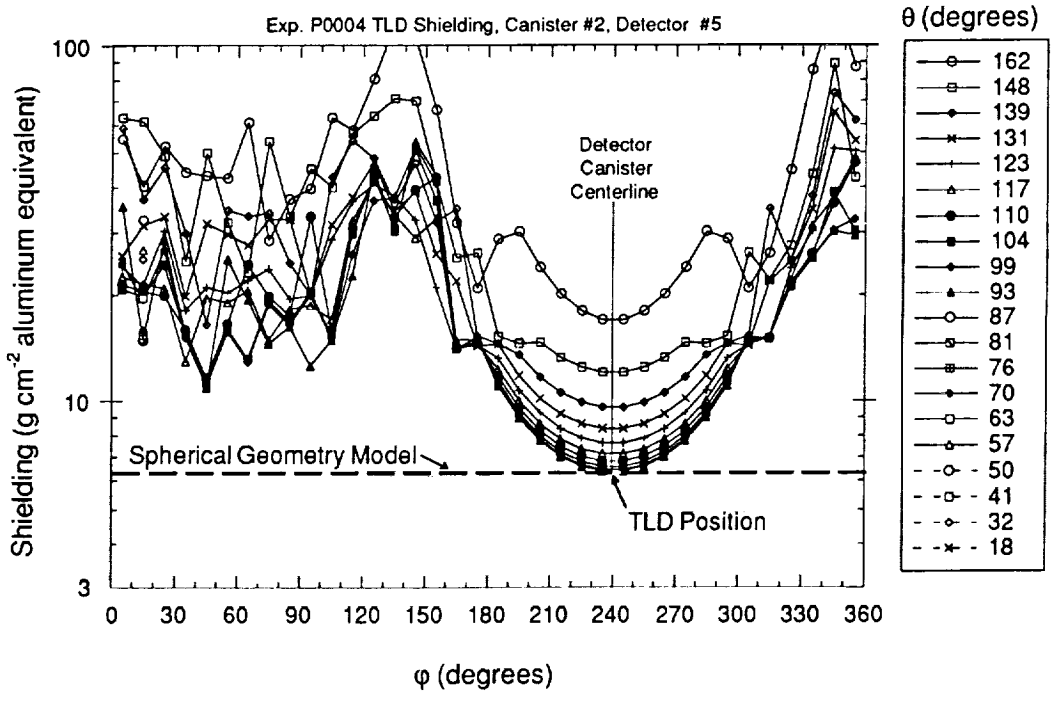

Figure 2. Example of shielding distributions generated using the 3-D spacecraft geometry model in predicting LDEF thermoluminescent dosimetry (TLD) response. Shown are areal densities along rays specified by the angles φ and θ (defined in text) emanating from a particular TLD location in the SEEDS experiment canister (Exp. P0004). The constant shielding for a simple 1-D spherical geometry model (used in some LDEF pre-recovery dose estimates) is shown for comparison.

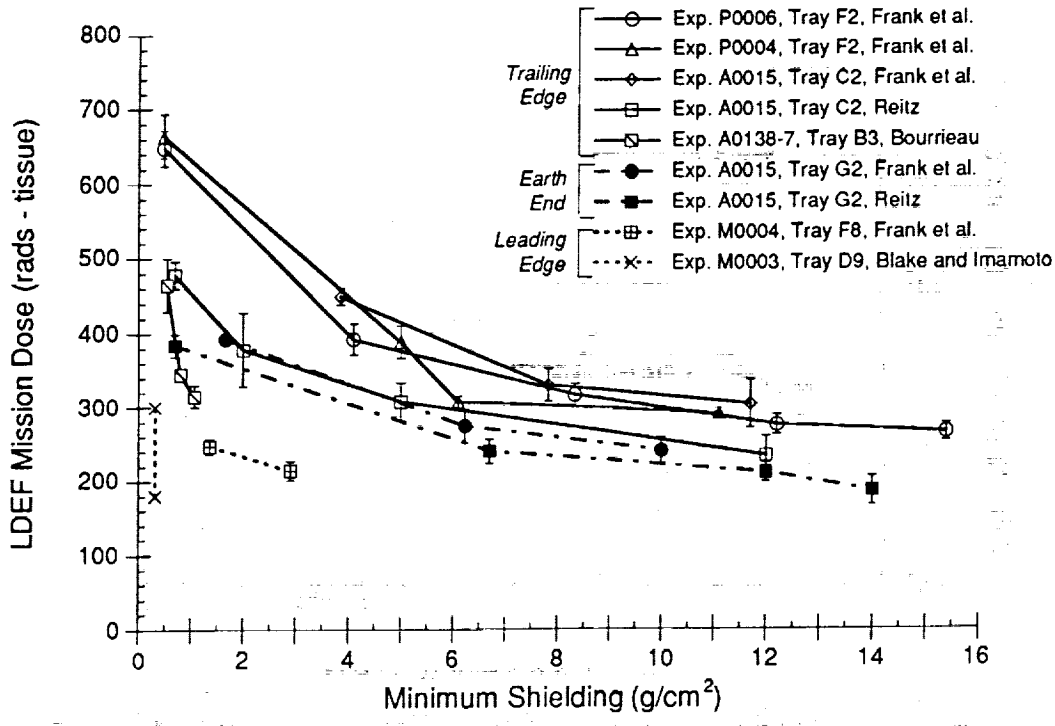

Figure 3. Summary of ionizing radiation dose measurements made on LDEF by thermoluminescent dosimeters (TLDs) at shielding depths where the dose is dominated by trapped protons.

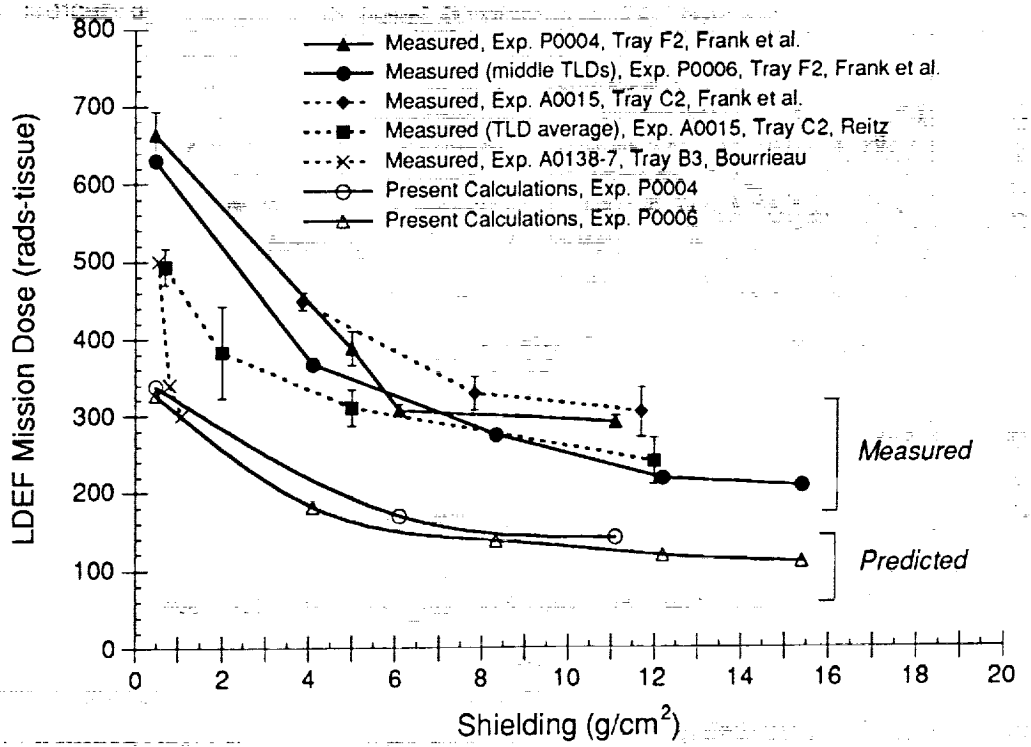

Figure 4. Predicted vs. measured radiation dose due to trapped proton environment for LDEF experiments on trailing (west) side of spacecraft.

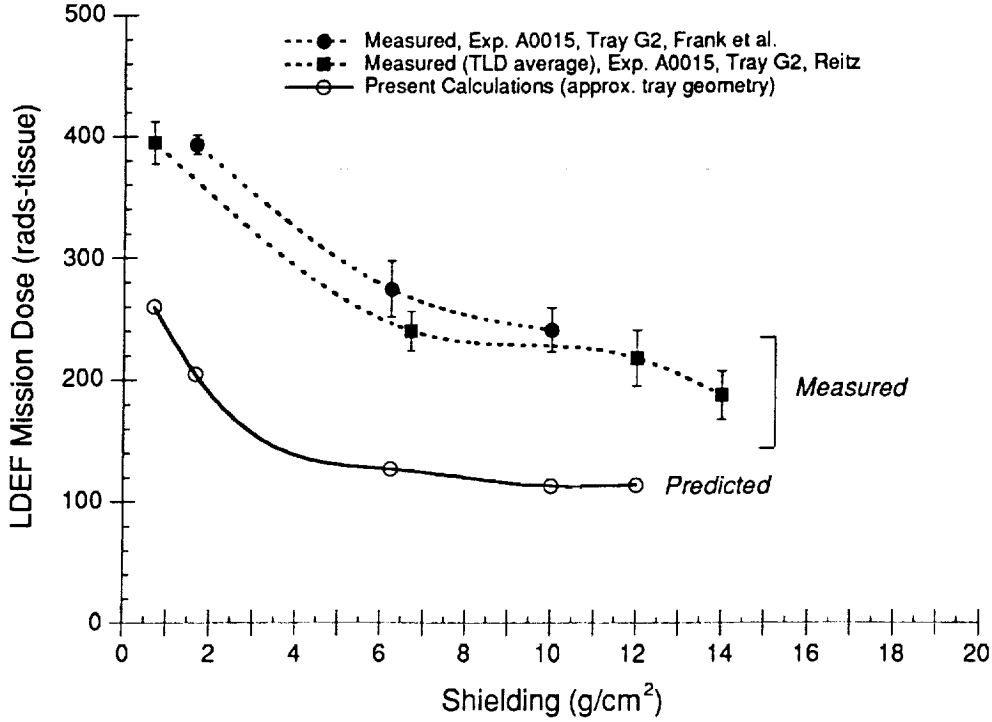

Figure 5. Predicted vs. measured radiation dose due to trapped proton environment for LDEF experiments on earth end of spacecraft.

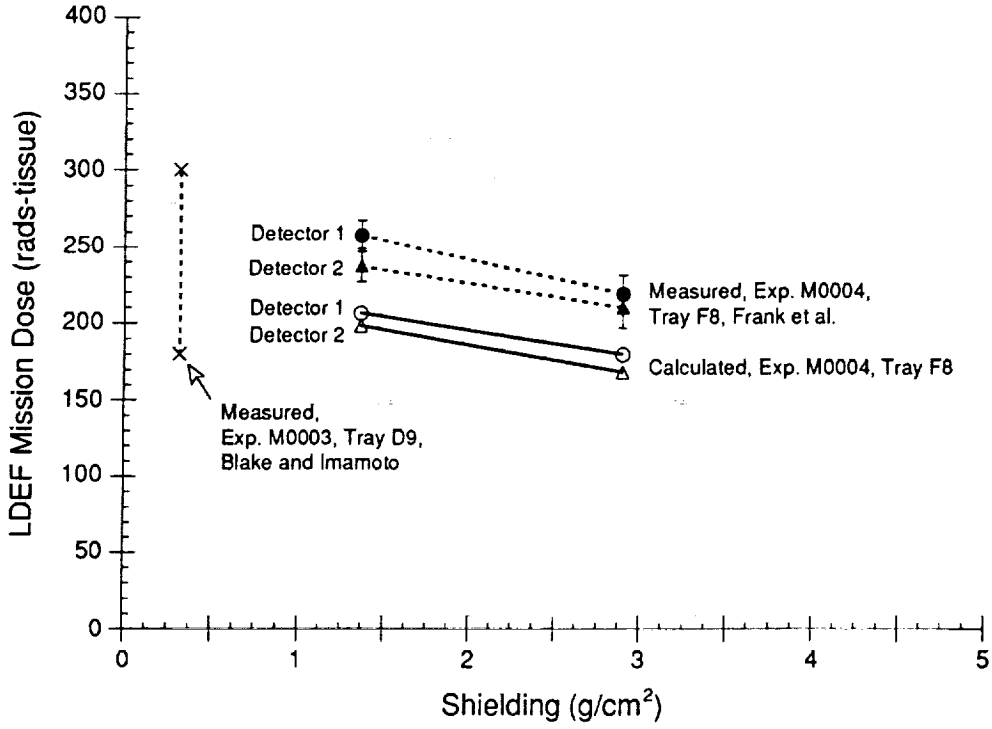

Figure 6. Predicted vs. measured radiation dose due to trapped proton environment for LDEF experiments on leading (east) side of spacecraft.

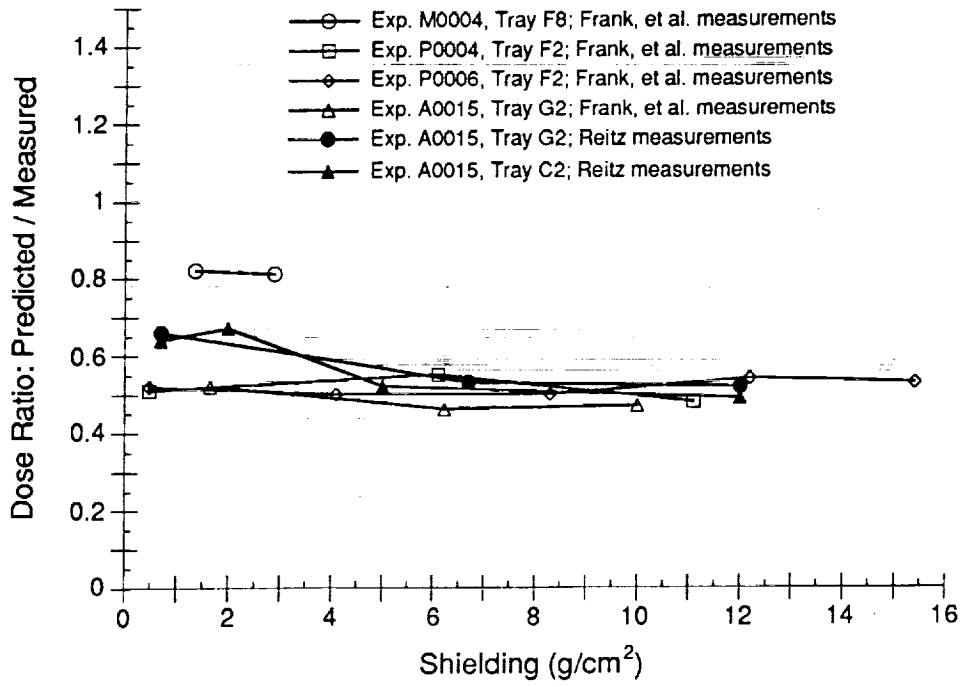

Figure 7. Ratio of predicted-to-measured radiation dose (in tissue) due to trapped proton environment based on LDEF data from thermoluminescent dosimeters.

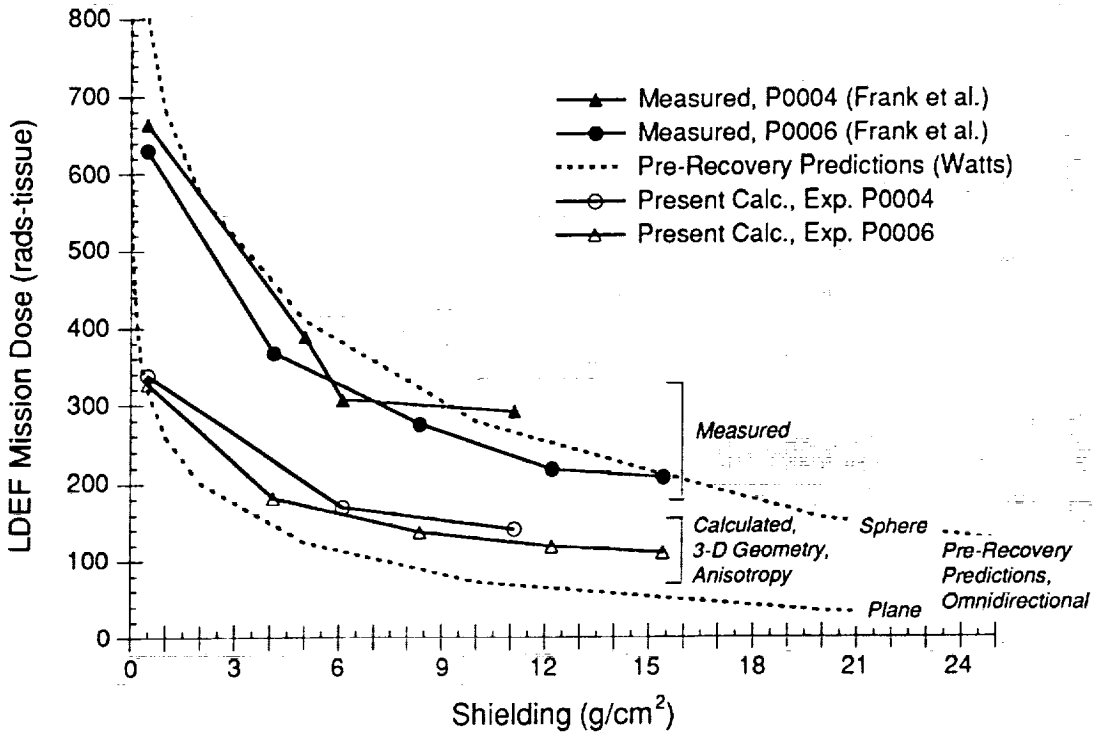

Figure 8. Influence of geomery model and environment anisotropy on predicting LDEF dose from trapped protons.

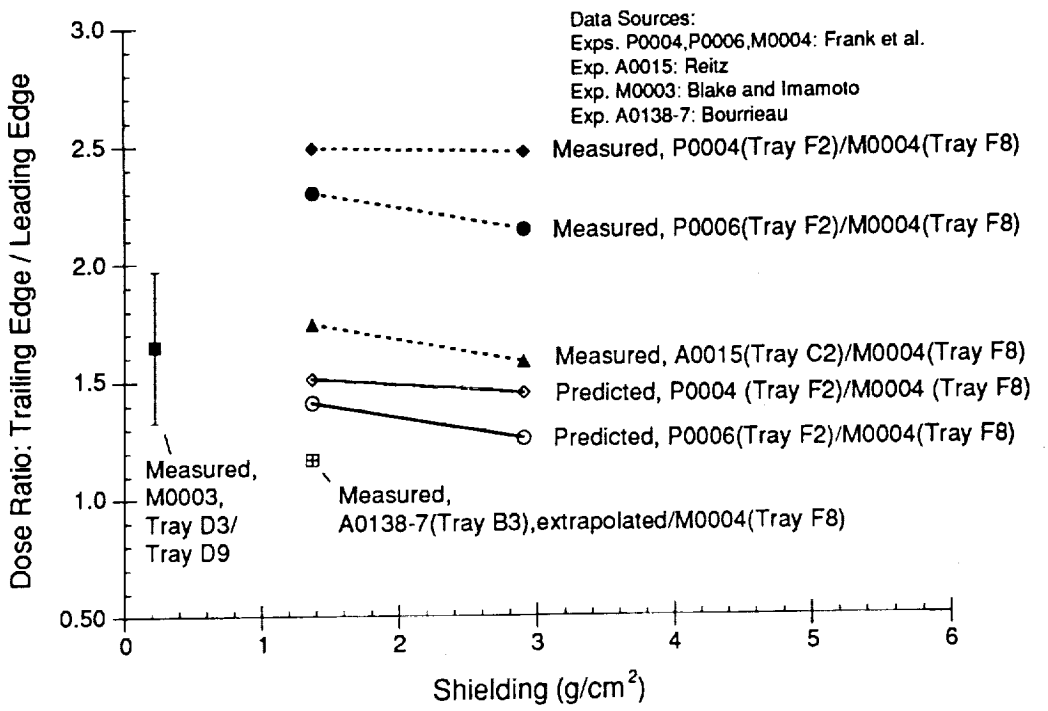

Figure 9. Radiation dose anisotropy on LDEF due to the directionality of the trapped proton environment. Shown are predicted and measured values of the ratio for the dose on the trailing (west) side LDEF to the dose on leading (east) side.

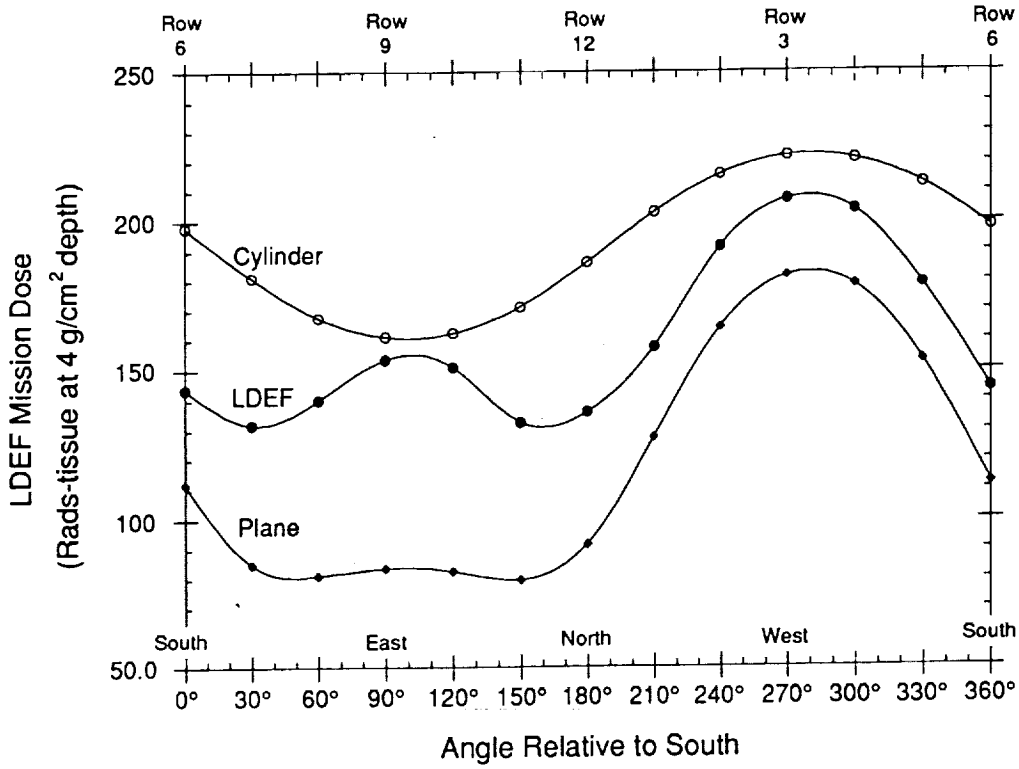

Figure 10. Influence of geomery model on predicted directionality of absorbed dose for LDEF mission due to trapped proton exposure.

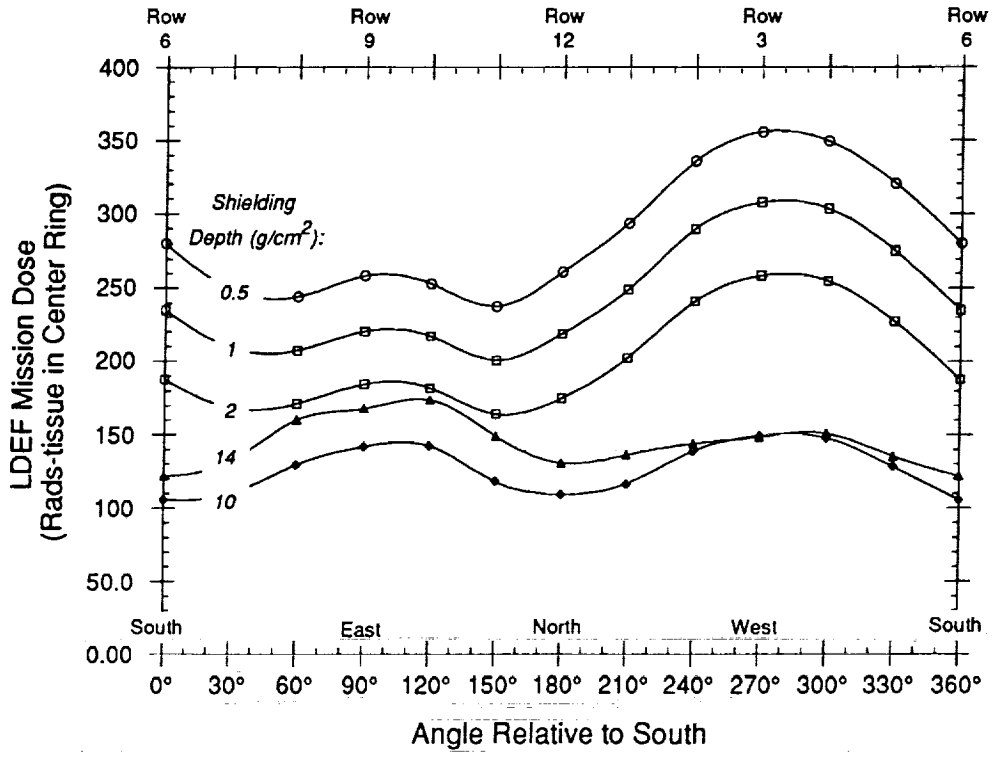

Figure 11. Influence of shielding depth on predicted directionality of absorbed dose from trapped protons. The dose is calculated in the center ring of the LDEF spacecraft using a 3-D geometry/mass model.

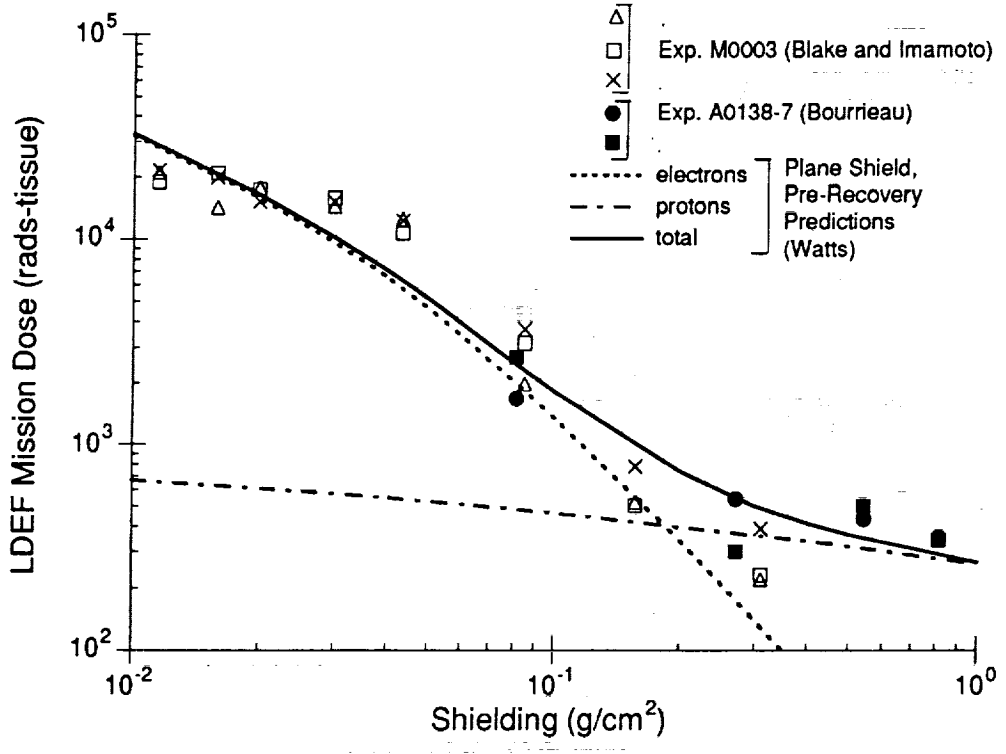

Figure 12. Comparison of measured and predicted absorbed dose for thermoluminescent dosimeters on LDEF having thin shielding where the dose is due to the trapped electron environment.